The Influence of Disturbance Dynamo Electric Field in the Formation of Strong Sporadic *E* Layers Over Boa Vista, a Low-Latitude Station in the American Sector

L. C. A. Resende[1,2] ID, J. K. Shi[1,3] ID, C. M. Denardini[2] ID, I. S. Batista[2] ID, P. A. B. Nogueira[4] ID, C. Arras[5], V. F. Andrioli[1,2] ID, J. Moro[1,6] ID, L. A. Da Silva[1,2], A. J. Carrasco[7], P. F. Barbosa[2,8], C. Wang[1] ID, and Z. Liu[1]

[1]State Key Laboratory of Space Weather, NSSC/CAS, Beijing, China, [2]National Institute for Space Research—INPE, São José dos Campos, Brazil, [3]National Space Science Center, University of Chinese Academy of Sciences, Beijing, China, [4]Federal Institute of Education, Science and Technology of São Paulo - IFSP, Jacarei, Brazil, [5]Helmholtz Centre Potsdam, German Research Centre for Geosciences (GFZ), Department 1: Geodesy and Remote Sensing, Potsdam, Germany, [6]Southern Regional Space Research Center—CRS/COCRE/INPE, Santa Maria, Brazil, [7]Departamento de Física, Universidad de Los Andes, Mérida, Venezuela, [8]Salesian University Center of São Paulo, Campus São Joaquim, Lorena, Brazil

Abstract This study analyzes strong sporadic *E* layer (Es) formation in Boa Vista (BV, 2.8°N, 60.7°W, dip: 18°), a low-latitude region in the Brazilian sector, which occurred far after the onset of a magnetic storm recovery phase. Such occurrences were observed during seven magnetic storms with available data for BV. Thus, the ionospheric behavior on days around the magnetic storm that occurred on 20 January 2016 was investigated to search for possible explanations. This analysis indicated that the probable mechanism acting during the Es layer strengthening is the zonal westward electric field caused by a disturbance dynamo. The same evidence was also observed in two other magnetic storms at the same location. Hence, a numerical model of the *E* region dynamics, called MIRE (Portuguese acronym for *E* Region Ionospheric Model), was used to confirm whether the disturbance dynamo could cause the Es layer intensification. The inputs for the model were the electric field deduced from the vertical drift and the wind components provided by GSWM-00 model. The simulations indicate that the Es layer density is significantly enhanced when the zonal electric field is present compared to the reference scenario with only the winds. Therefore, it is concluded that the disturbance dynamo electric field is the likely cause of the strong Es layers in the analyzed cases. Finally, the combined results from the model and observational data seem to contribute significantly to advance our understanding of the role of the electric fields in the Es layer formation at low latitudes.

1. Introduction

Sporadic *E* (Es) layers are dense and thin layers, which are mainly formed by the wind shear mechanism in low/midlatitudes (Haldoupis, 2011; Mathews, 1998; Whitehead, 1961). The metallic ions of meteoric origin are accumulated at the null points of the winds causing density enhancement at *E* region heights. Although these layers are named sporadic, they can be considered as permanent layers due to their frequent observation and the long lifetime of the metallic ions, such as Fe^+, Mg^+, K^+, Ca^+, and Na^+ (Kopp, 1997). Several authors studied the Es layer characteristics showing that their intensity and locations are controlled generally by the tidal wind atmospheric dynamics (Pignalberi et al., 2014; Prasad et al., 2012; Resende et al., 2017a) and, in some cases, by the electric field (Abdu et al., 2014; Moro et al., 2017; Resende et al., 2017b).

The ionospheric zonal electric field suffers significant modifications in equatorial and low-latitude regions during disturbed periods. These modifications/disturbances can be classified into two distinct categories: the prompt penetration electric fields (PPEFs) and the disturbance dynamo electric fields (DDEFs) (Balan et al., 2008; Blanc & Richmond, 1980). The electric field is related to the B_z component of the interplanetary magnetic field (IMF) and the solar wind velocity (V_{SW}) (Blanc & Richmond, 1980). During a southward incursion of IMF B_z, there is an undershielding electric field that penetrates the ionosphere with eastward polarity during the day and westward polarity during the night. An IMF B_z reversal to the north generates

an overshielding condition, leading to an electric field direction opposite to that of the undisturbed dynamo electric field (Nogueira et al., 2011). The DDEF occurs as a consequence of the energy input into the high latitude ionosphere. This interaction results in Joule heating and collisional interactions that drive disturbance thermospheric winds toward the equator, creating a DDEF. The DDEF generally occurs after the energy input at high latitudes, commonly during the later phases of the geomagnetic storms, and has the opposite direction to the quiet time electric fields (Santos et al., 2016).

Close to the geomagnetic equator, the electric field influence in the Es layer formation becomes more prominent since the wind shear is not a favorable mechanism in these areas (Arras et al., 2008). The irregularities in the *E* layers cause the nonblanketing Es traces observed on daytime ionograms at equatorial regions. They are classified as q-type Es or Es$_q$ and are the manifestation of the gradient drift instability in ionograms (Type II irregularities) due to the equatorial electrojet current (EEJ) (Abdu et al., 1996; Resende et al., 2016). Nevertheless, the Es$_q$ layers can disappear during disturbed periods when the neutral-dynamical process becomes efficient. Resende et al. (2013) performed a statistical analysis of the Es layer behavior during the magnetic storms of Solar Cycle 24 in an equatorial station. The results showed the occurrence of other Es layer types, mainly during the recovery phase of the magnetic storm, that is generally associated with wind shears. The observation of these types of layers is more common at low latitudes/midlatitudes than at equatorial regions. Therefore, they concluded that the polarization electric field inversion at the dip equator weakens the Type II irregularities.

Resende et al. (2016) used a modified model initially developed by Carrasco et al. (2007) to analyze the wind and electric field effects in the Es layer during quiet times. The results confirm that the winds are the principal mechanism of the Es layer formation at low latitudes, whereas the electric field plays a secondary role. Moro et al. (2017) used the same model to analyze the equatorial Es layer formation during the magnetic storm that occurred in November 2004. The results showed that the vertical electric fields of the EEJ irregularity inferred from coherent radar data can suffer severe changes, disrupting the Es$_q$ layers.

Abdu et al. (2003) showed the relationship between the Es layer occurrence/disruption and the evening prereversal enhancement (PRE) in the vertical drift (or electric field). During the disturbed periods, they observed high values of PRE, which disrupts the Es layers. Es layer disruption did not occur when the disturbance dynamo inhibits the PRE amplitude. Abdu and Brum (2009) performed a similar analysis for quiet periods. They concluded that the PRE development process is coupled with the Es layer formation in the evening at low latitudes. However, in both works, they stated that the electric field effect in the Es layer formation still needs more in-depth analysis.

More recently, Singh and Sripathi (2020) presented a statistical study on the equatorial spread *F* (SF) occurrence and its relation to the Es layers formation at low latitude during magnetic storms. They used two ionosondes, one located in an equatorial region and another located over an off-equatorial area. In most cases of their study, they observed a reduction of the Es layer frequency and height parameters (*fo*Es and *h'*Es) during the strong SF presence, mainly at low latitudes. Besides that, Batista et al. (2008) had already tried to find this same relationship between the SF occurrence and Es layer characteristics on Boa Vista (BV) during the Conjugate Point Equatorial Experiment (COPEX) campaign, which occurred in Brazil from October to December 2002. They concluded that the PRE with high amplitude, which is related to the SF, is too weak to affect the Es layer development. These differences between the observations in Batista et al. (2008) and Singh and Sripathi (2020) show that the Es layer formation dynamic has particularities in regions like BV and requires further studies to be fully understood.

Regarding the disturbed periods, some previous works connect the Es layer modifications with the undershielding/overshielding electric fields. Rastogi et al. (2012) studied the PPEF effect in the Es modification during a magnetic storm that occurred on 9 November 2004. They investigated the regions located around and away from the dip equator. The strong Es layers only occurred at low latitudes when the EEJ mechanism was not effective. They associated these layers, which occurred during the main phase of the magnetic storm, with the large westward PPEF penetrating the ionosphere.

Abdu et al. (2014) presented cases of Es layer formation/disruption during the development and growth phases of magnetospheric storms. The anomalous Es layers observed were associated with the Hall electric field induced by the zonal magnetospheric electric fields that penetrate the equatorial/low latitudes. These

modifications in the Es layers occur during or a few hours later of the magnetic storm beginning. When the penetration of the disturbed electric field occurs at evening/sunset times, the zonal eastward electric field (undershielding) can disrupt the Es layer, whereas the zonal westward electric field (overshielding) contributes to forming the Es layer. It is essential to mention that Abdu et al. (2014) analyzed regions close to the South Atlantic Magnetic Anomaly (SAMA) center, which intensifies the *E* layer conductivity and density, affecting the Es layer dynamics as well.

A digisonde DPS-4D is under continuous operation in BV (2.8°N, 60.7°W, dip: 18°). During normal conditions, the ionograms show weak Es layers because of the low wind amplitude, which is common in stations located close to the geographic equator such as BV. However, after the occurrence of a magnetic storm, we often detect strong Es layers, which are observed far after the recovery phase onset. These atypical Es layers in BV occur far after the recovery phase beginning of seven magnetic storms with data available. Since BV is not close to the SAMA center and because of the magnetic storm phase at which the Es layer is formed, the conclusions in Rastogi et al. (2012) and Abdu et al. (2014) cannot be readily applied.

In the present work, we selected the magnetic storm that occurred on 20 January 2016 to perform a case study, searching for a possible explanation for the unexpected Es strengthening. It was analyzed the *F* region parameters combined with the total electron content (TEC) maps from the Global Navigation Satellite System (GNSS), indicating that a DDEF event was the cause of the atypical Es layer. To further support this claim, we selected two additional storms at BV and analyzed the TEC maps, which provided evidence that the Es layer strengthening also occurred due to DDEF. In the sequence, a numerical model of the *E* region dynamics (MIRE—Portuguese acronym for *E* Region Ionospheric Model) (Resende et al., 2017a) was used to quantify the effect of the disturbed electric field in the Es layer formation. All the details concerning data analysis and calculations gave us an indication that these strong Es layers in BV are a consequence of the combined effect of the winds and disturbed electric fields, with the DDEF being the most probable cause. All these finds are presented in the following sections.

2. Ionospheric Data and Modeling

Data from digisonde (DPS-4D) were collected and analyzed to obtain information on *F* layer and Es parameters at BV and the following stations: Campo Grande (CG, 20.5°S, 55°W, dip: −17°), São Luís (SLZ, 2.5°S, 44.3°W, dip: −3.8°), and Fortaleza (FLZ, 4°S, 38°W, dip: −9°). We also analyzed the TEC data obtained from a network of GNSS receivers in South America to verify the response of equatorial and low-latitude ionosphere during a magnetic storm. Additionally, inputting the Global Scale Wave Model (GSWM-00) to MIRE, it was possible to study the electric field interaction with the Es layer dynamics for the intense geomagnetic storm of January 2016 in the selected Brazilian region. In the following sections, each set of data and the models used in this work are briefly described.

2.1. Digisonde Data

Digisonde is a radar that operates at frequencies ranging from 1 to 30 MHz. It generally operates continuously, making a complete sweeping every 10 to 15 min (Reinisch et al., 2004; Reinisch et al., 2009). The output data provide the ionospheric profile in graphs of frequency versus virtual height, from which it is possible to obtain the parameters for all the ionospheric layers. In this study we used the following parameters to perform the analysis: the Es blanketing frequency (*fb*Es), which corresponds to the frequency up to which the Es layer blocks the transmitted electromagnetic wave, and the top frequency (*ft*Es), which is the maximum frequency reflected by the Es layer. Furthermore, to study the magnetic storm effect in the ionosphere as a whole, we also analyzed the height of the *F* layer peak density (*hm*F2), and the vertical drift velocity (V_z).

The V_z is obtained by the relation $\Delta hF/\Delta t$, in which the *hF* was computed from the true heights at the specific plasma frequencies od 4, 5, and 6 MHz. This procedure is possible by using the mean drift values obtained at those frequencies, which represent the height-averaged vertical drift of the *F* region bottom side. More details about this methodology can be found in Abdu et al. (2010).

It is important to emphasize that we manually scaled all the ionospheric parameters using the SAO software (Reinisch et al., 2004) since significant discrepancies are often found between the automatically generated and real ionospheric parameters in the studied regions. Further information on the ionosonde, data

availability, and other parameters related to the ionospheric observatories from which we collected the data for this work can be found in the review by Denardini et al. (2016).

2.2. GNSS TEC Variation

The frequency radio signals from the GNSS receiver measures the total number of electrons (TEC) in a column of unitary cross-section area between the satellite and the receiver. The website of the Brazilian Studies and Monitoring of Space Weather (Embrace—http://www2.inpe.br/climaespacial/portal/en/) provides the TEC values that produce the ionospheric maps. Specifically, the two-dimensional maps of the absolute vertical TEC values with 10 min of time resolution and $0.5° \times 0.5°$ of spatial resolution in latitude and longitude were obtained for this analysis. Otsuka et al. (2002) developed this methodology, and Takahashi et al. (2016) applied it to the Brazilian sector.

2.3. MIRE Model

The Es layers were simulated using a theoretical model, called MIRE, which provides the E region electron density. The model solves a system of differential equations of the continuity and momentum for the molecular/atomic (NO^+, O_2^+, N_2^+, O^+) and metallic (Fe^+,Mg^+) ions. The system was solved using 0.05 km grid spacing in height and 2 min time step between 00 UT and 24 UT. In this analysis, we used the height range from 86 to 120 km. Notice that MIRE can be used for heights up to 140 km, but the GSWM-00, which is used in this work to compute the input winds for MIRE, does not provide data above 120 km. Carrasco et al. (2007) and Resende et al. (2017a) give more details about the equations and implementation of MIRE.

The vertical velocity of the ions that leads to the Es layer formation dynamics is given by Equation 1

$$V_{iz} = \frac{\omega_i^2}{(v_{in}^2 + \omega_i^2)} \left[\cos I \cdot \sin I \cdot U_X + \frac{v_{in}}{\omega_i} \cdot \cos I \cdot U_y + \frac{1}{v_{in}} \frac{e}{m_i} \cdot \cos I \cdot \sin I \cdot E_x + \frac{e}{\omega_i m_i} \cdot \cos I \cdot E_y + \frac{e}{v_{in} m_i} \cdot \left(\frac{v_{in}^2}{\omega_i^2} + \sin^2 I \right) \cdot E_z \right],$$

(1)

where ω_i is the ion gyrofrequency; v_{in} is the ion-neutral collision frequency; I is the magnetic inclination angle; m_i is the mass of the ion; e is the electric charge of the ion; E_x, E_y, and E_z are the electric field components; and U_x and U_y are the meridional and the zonal wind components in the E region. Here, the X axis points toward the south, the Y axis points toward the east, and the Z axis completes the right-handed coordinate system, pointing up.

In the previous studies that used MIRE (Moro et al., 2017; Resende et al., 2016; Resende et al., 2017a; Resende et al., 2017b), the authors fitted the wind model from the amplitude, wavelength, and phase parameters computed using the observational data of the meteor radars installed in Brazilian low-latitude regions. However, there is no meteor radar available near BV. Thus, in the present study, it was necessary to use a theoretical model for the winds. The GSWM-00 was selected because that model successfully describes the wind dynamics over the regions near to the geographic equator (Buriti et al., 2008; Hagan & Forbes, 2002, 2003). The website of the High Altitude Observatory (HAO) of the National Center for Atmospheric Research (NCAR) in Colorado (http://web.hao.ucar.edu/public/research/tiso/gswm/gswm.html) provides detailed information about the GSWM-00.

Using GSWM-00, the semidiurnal (12 hr) and diurnal (24 hr) amplitudes, the phase, and the wavelength for zonal and meridional tidal wind components in BV were obtained. Thus, the tidal components can be computed by

$$U_x(z) = U_{x0}(z) \cdot \cos\left(\frac{2\pi}{\lambda_x}(z - z_0) + \frac{2\pi}{T}(t - t_{x0}(z)) \right),$$

(2)

$$U_y(z) = -U_{y0}(z) \cdot \sin\left(\frac{2\pi}{\lambda_y}(z - z_0) + \frac{2\pi}{T}(t - t_{y0}(z)) \right),$$

(3)

where $U_{x0}(z)$ and $U_{y0}(z)$ are the wind amplitudes at the height z; λ_x and λ_y denote the wavelengths; T is the tidal period (24 hr for diurnal and 12 hr for semidiurnal); z_0 is a reference height, assumed as 100 km; and $t_{x0}(z)$ and $t_{y0}(z)$ are the wave phases.
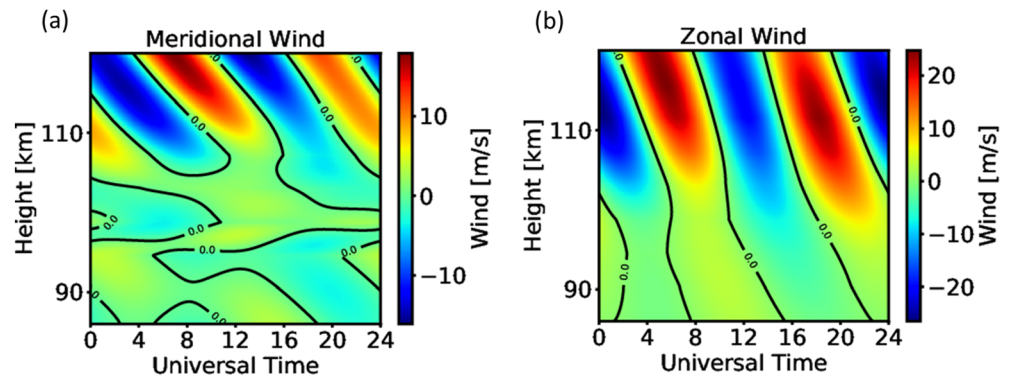
Figure 1. Wind profile of the (a) meridional and (b) zonal components obtained by GSWM that was included in MIRE to simulate the Es layers over BV.

Figure 1 shows the temporal and altitudinal variation of the meridional (Figure 1a) and zonal (Figure 1b) wind components of the tidal modes that were included in MIRE to simulate the Es layers over BV. Notice that the GSWM-00 was used as input in MIRE for the first time, requiring validation before performing the analysis of the electric field effects.

The null points (zero curves) indicate that the wind shear mechanism, which is necessary to form the Es layer, is cleared represented by the GSWM-00. The zonal amplitude is larger (max ~25 m/s) than the meridional amplitude (max ~17 m/s), which agrees with the observational results obtained previously for other Brazilian regions (Resende et al., 2017a, 2017b). However, the wind amplitudes are lower in BV than at other Brazilian regions analyzed before. Hence, weak Es layers are expected at BV in most days. This conclusion is in good agreement with the numerical results obtained from MIRE, as will be shown in section 3.

3. Results and Discussion

3.1. Magnetic Storm Event

Figure 2 shows the variation of the (a) IMF B_z component, (b) the solar wind speed (V_{SW}), (c) the Dst index, and (d) the auroral electrojet (AE) index for the 18–25 January 2016 geomagnetic storm period. The AE and Dst indices were obtained from the World Data Center from Geomagnetism in Kyoto, and the B_z and V_{SW} parameters from the OMNIWeb database, which, in turn, uses the measurements of the Advanced Composition Explorer (ACE) satellite.

The coronal mass ejection (CME) arrived in the Earth's magnetosphere on 19 January 2016 at 1000 UT, causing an abrupt increase of the B_z component. The CME effect lasted until 21 January 2016 when the Earth's environment started to recover. The B_z component turned southward (negative) from about 0530 UT on 20 January to 0400 UT on 21 January. The Dst index started to decrease (magnetic storm main phase) at around 0100 UT on 20 January, reaching almost −100 nT at 1600 UT. This value is the threshold for classifying it as an intense storm, according to Gonzalez et al. (1994). Afterward, it is possible to observe a slow recovery of the Dst index that lasted until 23 January. The V_{SW} increased gradually from about 320 to almost 600 km/s. The AE index showed a peak of ~1,250 nT around 1500 UT on 20 January. After this peak, the AE showed an oscillatory behavior, ranging from 200 to 500 nT.

3.2. Strong Es Layer in BV

During part of the magnetic storm recovery phase that occurred on 21–22 January 2016, we observed strong Es layers in BV, which differs from their typical behavior. The formation of this layer started at 2330 UT on 21 January, and it lasted until 0640 UT on 22 January, when it began to weaken (see the shaded area of Figure 2).

Figure 3 shows the ionograms registered in BV between 2350 UT on 21 January 2016 and 0750 UT on 22 January 2016, in increments of 1 hr. During this time, the *ft*Es oscillated between high and low values
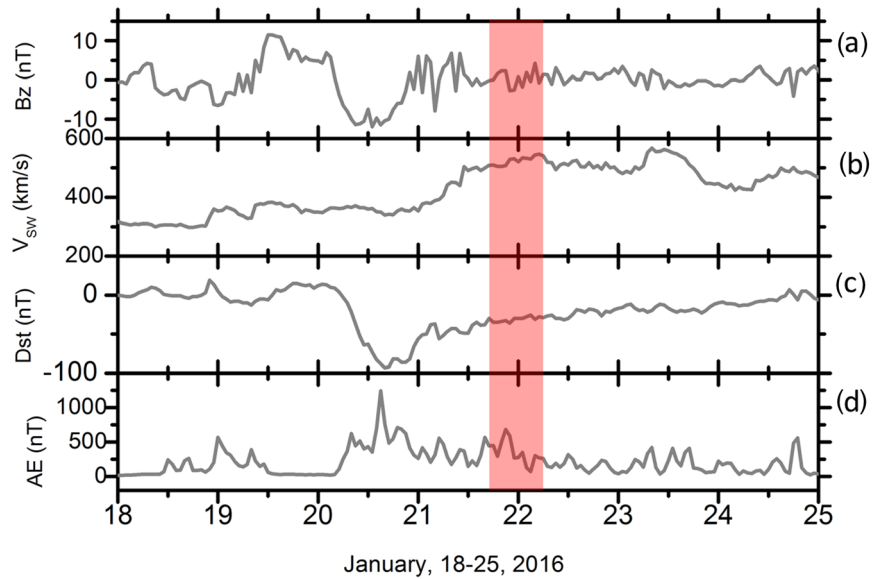
Figure 2. (a) IMF B_z, (b) solar wind speed, (c) Dst, and (d) AE auroral electrojet indices (UT) from 18 to 25 January 2016. The red bar refers to the period in which the strong Es layers are observed.

(red arrows in the figure). Between 2350 UT and 0130 UT, the ftEs reached values even higher than 15 MHz (e.g., see 0050 UT). After, the Es layer started to weaken (0150 UT), but it strengthened again in the next hours (see 0450 UT). This oscillation lasted until 0900 UT when the strong Es layer began to disappear. In the hours following 0900 UT, the Es layers returned to its typical behavior with a not significant density
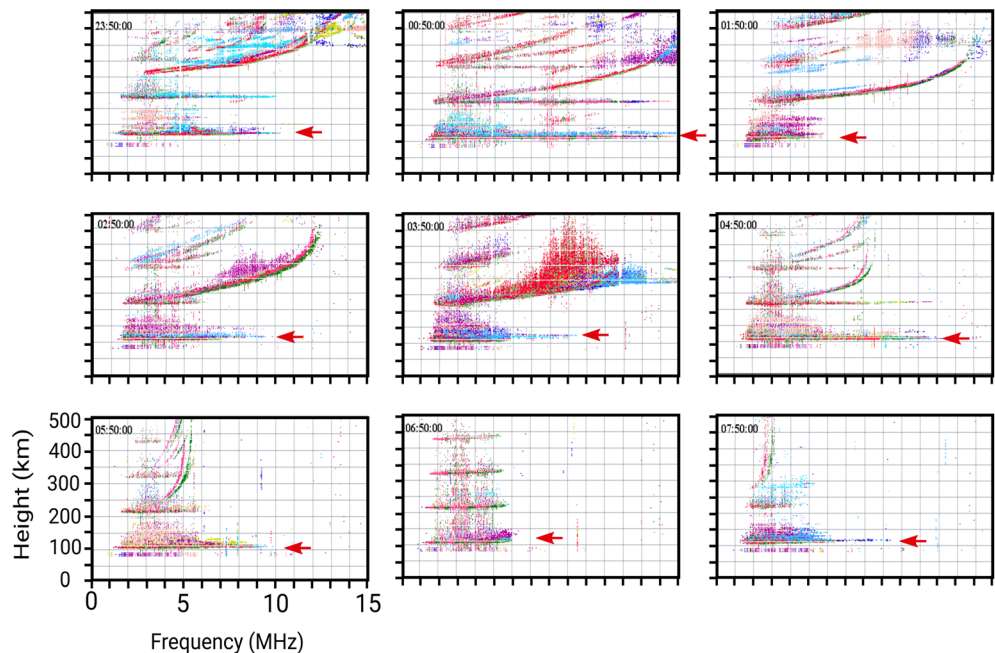

Figure 3. Ionograms at Boa Vista collected from 2350 UT on 21 January 2016 until 0750 UT on 22 January 2016, showing the atypical strong Es layers, indicated by the red arrows.

Table 1
List of Strong Es Layers in BV Associated to Moderate/Intense Magnetic Storms (Dst < −50) in 2016 and 2017

Arrival of the CME on Earth		Minimum Dst (nT)	Stronger Es layer observation		Maximum $ftEs$ (MHz)
5 March 2016	1900 UT	−98	8 March 2016	0050 UT	6.70
13 October 2016	0600 UT	−104	15 October 2016	2350 UT	8.72
3 November 2016	1800 UT	−50	4 November 2016	0000 UT	11.45
10 November 2016	0000 UT	−59	12 November 2016	2010 UT	9.49
27 May 2017	2200 UT	−125	30 May 2017	2030 UT	12.92
16 July 2017	1500 UT	−72	17 July 2017	2310 UT	6.20

(not shown here). In the supporting information to this manuscript, we provide a movie with all the ionograms available for the period from 2330 UT on 21 January to 1000 UT on 22 January 2016.

Other moderate/intense magnetic storms (Dst < −50) due to CME arrivals that occurred in 2016 and 2017 were also analyzed, a period with data available for the BV region. In all cases, as shown in Table 1, similar strong Es layers are observed in BV ionograms during the recovery phase (see the maximum of the $ftEs$ parameter). As will be discussed later, these layers cannot be only formed by wind shear mechanism since the tidal winds in the regions near the geographic equator, as BV, have small amplitudes in their meridional and zonal components (Figure 1). Therefore, another mechanism must be acting in this region to form these strong layers.

Motivated by this abnormal Es layer behavior at BV, we searched for strong Es layers in the data collected in other regions aiming to define the geographical/geomagnetical extent of such phenomena. Figure 4 shows the $fbEs$ (green line) and $ftEs$ (orange line) parameters between 21 and 23 January 2016, for four different low-latitude regions in Brazil: BV, CG, FLZ, and SLZ. The FLZ and SLZ are regions close to the magnetic equator, whereas CG is located at the same magnetic meridian as BV but in the Southern Hemisphere. From this figure, it is clear that the unusual high top frequencies of the Es layer, that is, the unexpected high electron densities, were only observed in BV. For the FLZ and SLZ regions, the $ftEs/fbEs$ during the nighttime had low values, disappearing after a few hours.

Since there are no wind measurements in these regions (SLZ and FLZ), and GSWM-00 output does not show enough wind shears to form Es layers, the Es layer modeling at the Brazilian regions faces some difficulties.
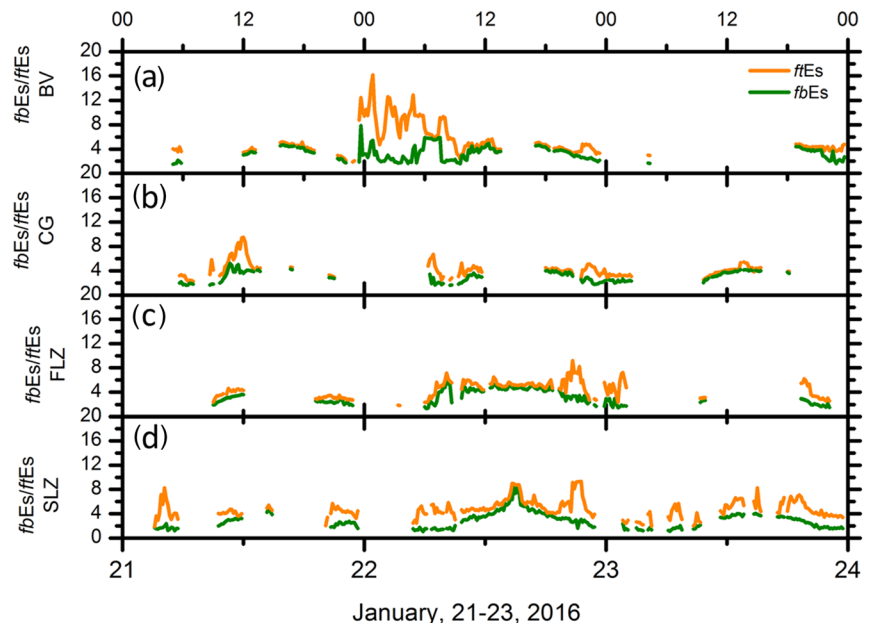

Figure 4. The $fbEs$ and $ftEs$ parameters on 21–23 January 2016 at two Brazilian low-latitude regions: Boa Vista (a) and Campo Grande (b), and at two Brazilian equatorial regions: Fortaleza (c) and São Luís (d).

Nevertheless, we recall that Resende et al. (2017b) studied the wind behavior to form Es layers using an all-sky interferometric meteor radar installed in São João do Cariri (7.23°S, 36.32°W, dip: −22.16°), the nearest region to São Luís with data available. They observed that the Es layer electron density in São Luís has low values during the day, disappearing in the night hours. This behavior agrees with the observations on SLZ and FLZ in the period analyzed here. Furthermore, the authors concluded that the zonal wind component is the most crucial driver in the Es layer formation. This component close to the magnetic equator has low amplitudes, which yields the formation of weak Es layers. In some hours for these regions, the fbEs showed a typical behavior characterized by an enhancement during the morning period, starting about 09 UT (06 LT), and reaching maximum values about 15 UT (12 LT), followed by a steady decrease, reaching the quiescent values after 21 UT (18 LT) (Resende et al., 2017a). Given all these facts, it is concluded that the Es layers in SLZ and FLZ do not have any atypical behavior, as observed in BV.

Regarding CG (Figure 4b), the Es layer completely disappeared at the moment of the strong Es layer occurrence in BV. CG is located at the same magnetic meridian as BV, meaning that the integrated field line conductivity is the same in both regions (Abdu, Batista, et al., 2009). Batista et al. (2008) studied the relationship between the SF occurrence and Es layer characteristics. They used simultaneous data to search for any possible connection between these two phenomena in BV, CG, and Cachimbo (9.8°S, 54.5°W, dip: −4.2°). The COPEX campaign, which occurred in Brazil from October to December 2002, provisionally installed several instruments in these stations. They did not detect any significant correlation between the SF occurrence/generation at the magnetic equator and the presence of Es layers at the conjugate E regions along the same field line. However, they observed that the Es layers were stronger in BV when compared to those detected in CG. Nevertheless, they did not study the effect of the Es development or disruption with the vertical equatorial electric field, which is associated with the eastward electric field PRE.

Lastly, the digisonde installed in BV allows the analysis of the recurrent atypical Es layer during the recovery phase of the magnetic storm. In this context, we performed an in-depth study of the magnetic storm period in January 2016 to find a possible explanation of such behavior in BV. Our conclusions can be seen in the following sections.

3.3. The F Region Behavior

Figure 5a presents the F2 layer peak height (hmF2) parameter on 21 and 22 January 2016 over BV. The blue line refers to a quiet day (18 January) used as a reference. An important characteristic observed in this figure is that the *F* layer peak height enhancement near sunset (shaded area) was reduced when compared to the quiet period. The possible causes for this hmF2 reduction can be (1) a northward meridional wind which contributes to the lowering of the layer, (2) an eastward electric field reduction through an overshielding effect of a PPEF, or (3) a westward DDEF.

Figure 5b shows the difference between hmF2 measured at CG and BV (dhmF2 $= hm$F2$_{\text{CG}} - hm$F2$_{\text{BV}}$). As discussed in Abdu, Batista, et al. (2009) and Batista et al. (2017), dhmF2 is a measure of the interhemispheric symmetry/asymmetry in hmF2. Positive or negative values of dhmF2 indicate transequatorial meridional wind (TMW) directed northward or southward, respectively. At the time of the hmF2 reduction over BV, dhmF2 is negative, which means a southward TMW. Such a TMW would contribute to increasing the *F* layer height over BV, which was not observed in the data. The second hypothesis of an overshielding PPEF would occur under the presence of northward turning of the IMF-B_z, which was not observed during the time interval under consideration either. Moreover, B_z was close to 0, and AE presented minor fluctuations (see Figure 2), meaning that the overshielding PPEF hypothesis is unlikely. Therefore, it was concluded that a westward DDEF is the most probable candidate to explain the reduction in the rise of *F* layer peak height during the time of interest for this study.

To confirm the DDEF effect in the *F* layer height, the $E \times B$ drift was computed during the hours when the strong Es layers occurred. However, it is paramount to notice that the relation ($\Delta hF/\Delta t$) is only valid to obtain the vertical drift velocity near sunset and night hours when the *F* layer height is equal to or higher than 300 km (Bittencourt & Abdu, 1981). If the layer is below this height, then the recombination processes need to be taken into account for the drift velocity calculation, leading to
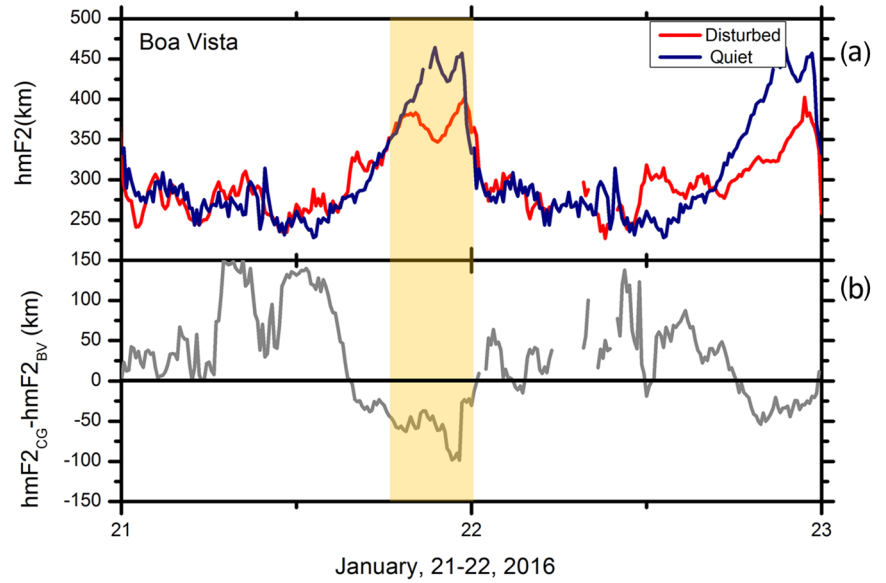
Figure 5. The hmF2 parameter at Boa Vista (a) and the difference between hmF2 in Campo Grande and Boa Vista (b) on 21–23 January 2016.

$$V_{BV} = V_{ap} - \beta H, \tag{4}$$

where the V_{BV} refers to the drift velocity at BV, V_{ap} is the apparent vertical drift (measured) for a station, β is the recombination coefficient, and H is the scale height of ionization. The recombination coefficient is given by

$$\beta = k_1[N_2] + k_2[O_2]. \tag{5}$$

Nogueira et al. (2011) provide the reaction coefficients k_1 and k_2, and the atmospheric model MSISE-90 (Hedin et al., 1991) was used to obtain the neutral molecular nitrogen and oxygen number densities, represented, respectively, by $[N_2]$ and $[O_2]$.

For stations located outside the magnetic equator, like BV, we need to consider the meridional wind since this component may contribute to the vertical plasma motion as well (Nogueira et al., 2011; Rishbeth et al., 1978). Therefore, V_{ap} is given by

$$V_{ap} = V_D \cdot \cos I \pm U_F \cdot \cos I \cdot senI - w_D \cdot \sin^2 I, \tag{6}$$

where V_D is the vertical drift velocity computed as $\Delta h\Delta/t$, I is the magnetic inclination angle (~18° in BV), U_F is the meridional wind component in the F region (positive northward), w_D is the contribution to the vertical plasma velocity due to diffusion, which is given by $w_D = g/v_i$, g being the gravity acceleration, and v_i is the ion-neutral collision frequency. We used the same methodology described in Nogueira et al. (2011) to compute v_i:

$$v_i = 4.34 \times 10^{-16}[N_2] + 4.28 \times 10^{-16}[O_2] + 2.44 \times 10^{-16}[O], \tag{7}$$

where $[N_2]$, $[O_2]$, and $[O]$ were also obtained from MSISE-90.

Figure 6 shows the vertical drift computed according to Equation 4. The gray line in the figure refers to the quiet period drift, whereas the orange line refers to the recovery phase of the magnetic storm,
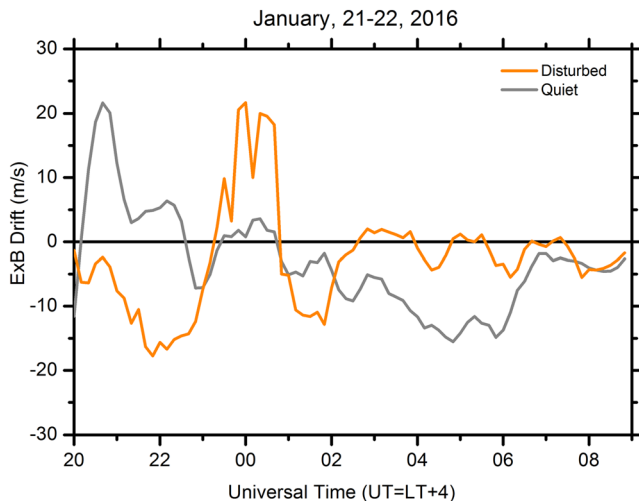

Figure 6. The $E \times B$ drift in quiet (gray line) and disturbed (orange line) periods between the 2000 UT and 0900 UT at Boa Vista on 21–22 January 2016.
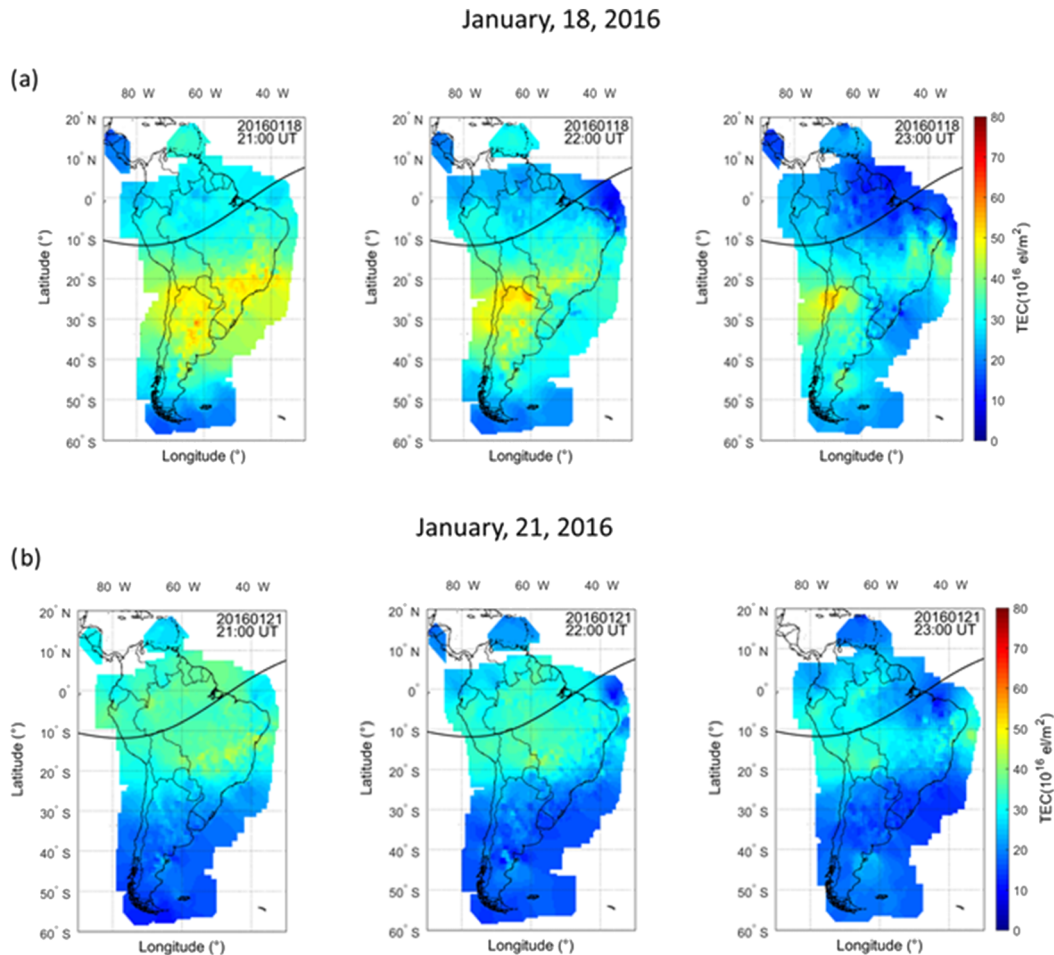
January, 18, 2016

January, 21, 2016

Figure 7. Longitude versus latitude distribution of the TEC map over South America at 1 hr interval (a) during the quiet time period and (b) covering the period of the disturbance dynamo effect. The color shows the TEC values.

which is called disturbed period. Positive drift values mean that it points toward the east, whereas negative drift values mean that it points toward the west. The DDEF effect during the PRE hours (2100 UT) is clearly seen as the strong inhibition of the $E \times B$ drift. During the quiet period, the $E \times B$ drift was positive between ~2015 UT and 2230 UT, with a peak value higher than 20 m/s. For the disturbed day, the drift was negative at the same time, reaching a value of less than −15 m/s. After these hours, the drift velocity tried to recover and reached values higher than that of the quiet drift velocity. Finally, after 0200 UT, the drift velocity presented an oscillatory behavior, showing that the drift was returning to the typical values.

Although Figure 6 presents the $E \times B$ drifts starting at 2000 UT of 21 January, we have analyzed the parameter for the entire day and observed that it presented low values of downward disturbance drifts between 0700 and 1700 LT, followed by more significant downward drifts near sunset and upward drift near midnight. The local time and seasonal dependence of the disturbance dynamo drifts are strongly anticorrelated with those of the drifts caused by undershielding PPEF as well as with the quiet time drift (Fejer et al., 2008). This anticorrelation seems to agree with the results presented in Figure 6, corroborating our assumption that the DDEF indeed occurred during the recovery phase of the analyzed magnetic storm.

The equatorial ionization anomaly (EIA) modification was also analyzed using TEC maps over South America to observe and confirm the presence of the DDEF effect. Figure 7 shows the TEC over South America. The solid black line across the map indicates the magnetic equator position in 2016. Figure 7a presents the TEC map during the reference quiet day (18 January 2016). Notice that the EIA southern crest is well demarked at low latitudes (yellow colors in maps) between 2100 UT and 2300 UT, which is the typical behavior of the ionosphere plasma over Brazil. The TEC Map on 21 January 2016 shows an apparent
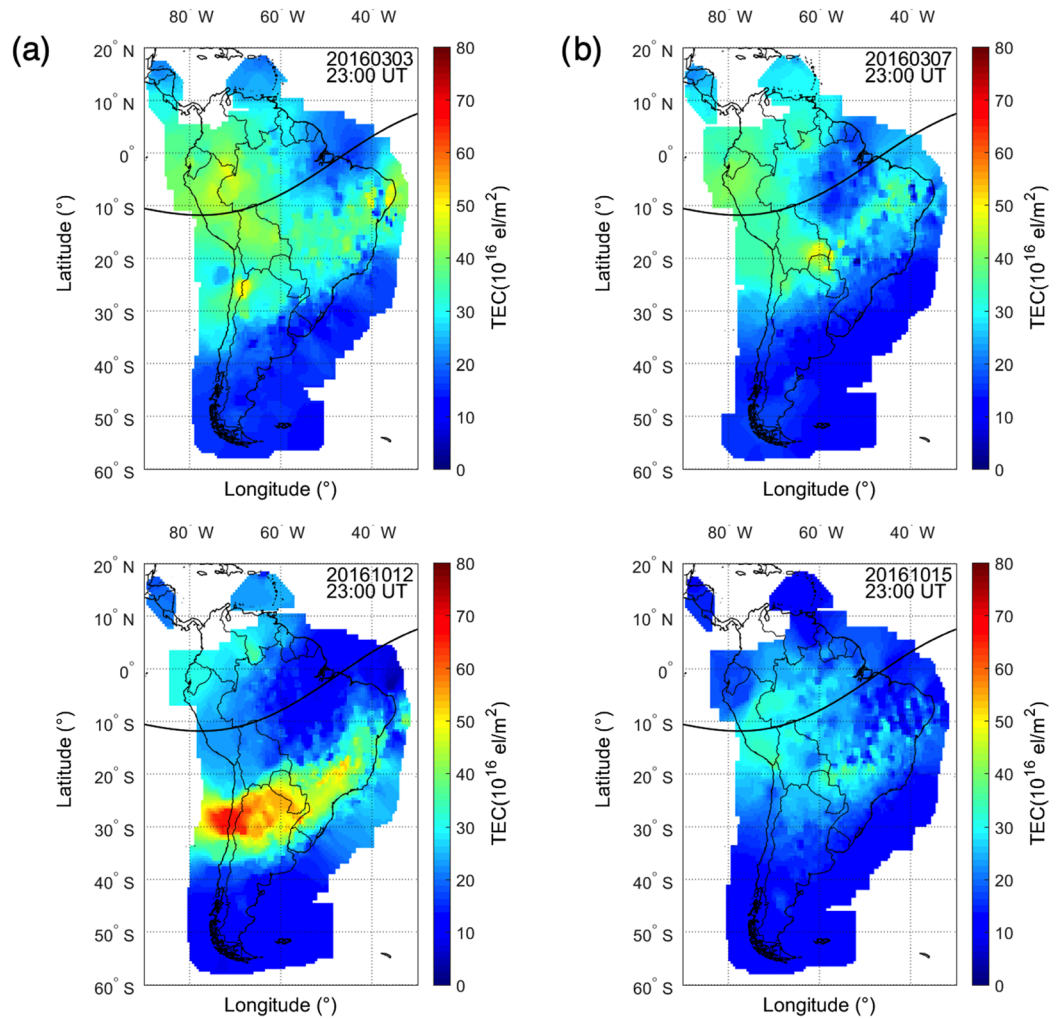
Figure 8. Longitude versus latitude distribution of the TEC map over South America at 23 UT (a) during the quiet time period just before the DDEF effect and (b) during the day when the DDEF effect is observed. The color indicates the TEC intensity.

weakening of the EIA crest near sunset time (Figure 7b). Nogueira et al. (2011) observed similar behavior, in which they analyzed the response of the ionosphere during two magnetic storms that occurred in 2001. That study analyzed the EIA intensity and the variations in the zonal electric field in different phases of the magnetic storms. They found that the PPEF mechanism occurred during the main phase in both cases, causing an enhancement in the EIA. However, during the recovery phase, they found that the DDEF almost caused an EIA crest disappearance, agreeing with our results.

Notice that this mechanism is a global phenomenon. Thus, the westward electric field in PRE hours due to disturbance dynamo occurs in all regions of Brazil, being more visible in those near the magnetic equator.

To further support our claim that the DDEF is the probable cause of the Es layer strengthening, two of the six events shown in Table 1 were analyzed: 8 March 2016 and 15 October 2016. Figure 8 shows the TEC maps over South America for those events. The left panel (a) refers to the reference quiet day at 23 UT (19 LT in BV) for each case (3 March 2016 and 12 October 2016), showing the EIA southern crest in yellow and greenish colors. The right panel (b) shows the TEC maps at the same UT for the days in which the atypical Es layer was observed. In both cases, the apparent weakening of the EIA is seen, confirming the presence of the DDEF effect around the hours that the strong Es layer occurred.

Therefore, on the light of the above discussion, the inhibition of the PRE drift and EIA are concrete evidences of the a DDEF influence that occurred in the recovery phase of these magnetic storms, as already
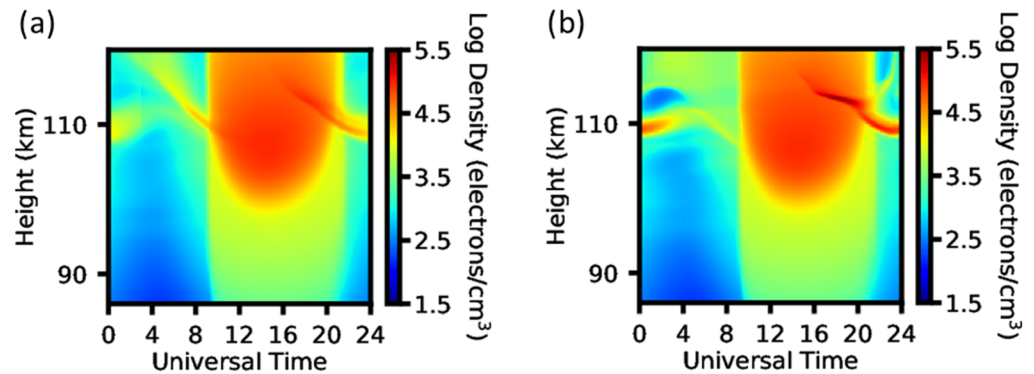
Figure 9. Electron density as a function of Universal Time (UT) and height (km) simulated by MIRE considering (a) the diurnal and semidiurnal tidal winds in January 2016 and (b) also the westward zonal electric field component of 0.5 mV/m.

discussed by several authors (Abdu, 1997; Abdu et al., 2006; Santos et al., 2012; Sastri, 1988). Thus, we infer that the DDEF can influence the strong Es layer formation on BV. This assumption, which has not been verified yet by the previous studies, is analyzed in the following section by comparing the observational data with the simulation results obtained by MIRE.

3.4. Analysis of the Electric Field Effect Using Simulations

In this work, we point out that the most probable mechanism to form the strong Es layers in BV is an electric field superposed to the wind shear mechanism. According to Fejer and Scherliess (1995), a variation of 1 mV/m in the zonal electric field leads to a variation of approximately 40 m/s in the vertical drift. From Figure 6, the drift during the hours of the PRE was approximately −20 m/s, which corresponds to a westward electric field of 0.5 mV/m. Comparing with the ionograms in Figure 3, it is observed that the strong Es layer was formed at 2350 UT, shortly after the electric field has reached its highest value. Later, the Es layer tried to return to normal conditions, around 0150 UT, when the fbEs and ftEs reached the lowest values in this period. At the same time, the drift velocity on 22 January 2016 showed a positive value of ~15 m/s, corresponding to an eastward electric field of approximately 0.42 mV/m. However, at 0400 UT, the drift velocity became negative; that is, the zonal electric field is westward again. At 0450 UT, the ftEs reached values around 13 MHz, but this behavior did not last long since the vertical drift oscillated in the following hours. Thus, this result shows a possible connection between the westward electric field and the Es layer formation. To confirm this hypothesis, simulations using MIRE were performed with these electric field values, as shown in the following.

First, we considered only the effect caused by the wind profile computed using the GSWM-00 on 22 January 2016 over BV. Figure 9a shows the Height-Time (HT) maps of the electron density profile simulated by MIRE (color scale). The background color maps show a typical behavior of the E region electron density, with low values in the night period and expressive electron density in the daytime. Notice that MIRE successfully simulated the Es layers, which are the thin descending layers observed in some hours. The Es layer formation occurred around 110 km with low density, and it presented a downward movement, agreeing with the theory about the Es layer dynamics (Bishop & Earcle, 2003; Haldoupis et al., 2006). This scenario shows a typical Es layer formed by the wind shear mechanism (Resende et al., 2017b). Notice that the Es layer did not seem to occur during the daytime since its density was very close to the background E region density. However, in the nighttime, which is our interest in this study, the Es layers were observed.

In the following, we included a constant westward electric field equal to 0.5 mV/m between 2000 UT and 0600 UT that corresponds to the PRE vertical drift of −20 m/s. Figure 9b shows the HT maps of the electron density profile simulated by MIRE for this scenario. It is possible to observe that the Es layer formed during the night hours were stronger than that of the reference scenario in Figure 9a. Furthermore, during the first hours of the morning (0000 UT until 0400 UT), the Es layer density when considering the constant electric field reached almost 10^5 electrons/cm^3, whereas the Es layer formed only by the winds reached a density of

approximately 10^4 electrons/cm^3. Therefore, the constant westward electric field strengthened the Es layers in BV.

Resende et al. (2016) and Moro et al. (2017) showed that the zonal electric field can cause a modulation in the existing Es layers because of the tidal wind mechanism. They studied the equatorial region electric field created by the EEJ current to analyze the Es layer formation, concluding that the zonal electric fields are not efficient enough to create or disrupt the Es layers. The only observable effect is some modulation. Therefore, the conclusions in this work are in agreement with those previous studies since the simulation results confirm that the electric field caused some variation in diurnal times.

Carrasco et al. (2007) analyzed the vertical electric field influence in the Es layers during the *F* region PRE by mapping these electric fields through the equipotential magnetic field lines to the *E* region heights. Depending on the vertical electric field direction, they observed an Es layer disruption or enhancement around the sunset and its correlation with the PRE. On the other hand, Abdu et al. (2014) investigated some similar modifications in the Es layers at low-latitude regions during magnetic storm periods. They showed that a PPEF of an overshielding electric field with westward polarity in the evening sector can form sporadic *E* layers near 100 km. They concluded after a careful analysis that the enhanced ratio of the field line integrated Hall to Pedersen conductivity ($\sum$H/$\sum$P) during the magnetic storms drove the Es layer intensification. Afterward, the vertical electric field is mapped to the *E* region, which can form strong Es layers. To confirm the enhancement of the $\sum$H/$\sum$P ratio, they selected stations located in the SAMA since the energetic particle precipitation mechanism is effective. They concluded that the electric field effects on Es layers occur more in the SAMA region during the disturbed periods.

In the present study, it was not possible to analyze the influence of the *F* region vertical electric field mapped to BV since there are no measurements at equatorial regions for the same magnetic field line. The absence of Es layers in CG indicates that this can be a possible mechanism. The vertical electric field can be mapped to BV and CG in opposite directions, causing, respectively, a strengthening and disruption of Es layers. However, the conclusion in Abdu et al. (2014) about the enhancement in the $\sum$H/$\sum$P ratio in SAMA regions is not possible here since BV is located far from the anomaly center. Thus, some other mechanism must be acting to account for the strong Es layers observed.

The literature (Fürst et al., 2009; Ginet et al., 2007) shows that the BV region lies on the SAMA northwest boundary, which means that this region may receive a few influences of the particle precipitation. Da Silva et al. (2016) presented the most probable particle precipitation region on the SAMA. They analyzed the X-Ray (3.0–31.5 keV) distribution of the upper atmosphere measured by the X-Ray Spectrometer (RPS) - device on board of the CORONAS-F satellite. The results indicated that there is no particle precipitation over BV. Even knowing that there is little chance of charged particle precipitation in the region of interest, it is crucial to investigate the dynamic processes on the outer radiation belt during our specific case study (2200 UT to 0000 UT on 22 January 2016), as shown below.

The Van Allen Probes data (Mauk et al., 2012) showed that the outer radiation belt flux (high-energy, figure not shown) for this event is considerably stable, that is, without dropout or enhancement. The data also showed the absence of the chorus (from hundreds of Hz up to about 10 kHz) and electromagnetic ion cyclotron—EMIC (0.3 Hz up to 3 Hz) wave activities. It means that the pitch angle scattering mechanism (Kennel & Petschek, 1966; Thorne, 2010) did not occur. Consequently, charged particles were not launched in the loss cone, resulting in the absence of particle precipitation during all periods of this case study. In the light of these conclusions, it is highly probable that the Es layers detected here formed without the particle precipitation influence. Therefore, the $\sum$H/$\sum$P enhancement, which intensifies in the SAMA region during the magnetic storms, has little or no impact on the mechanisms capable of strengthening the Es layers in the BV region.

Additionally, the Es layer intensification analyzed in Abdu et al. (2014), which was caused by a westward electric field, occurred during the overshielding processes. In our studies, on the other hand, the most probable mechanism acting during this magnetic storm is the DDEF effect. The fast variation of the electric field from eastward to westward on the night of 21–22 January 2016 might be causing the oscillations in the frequency parameters observed in Figure 3. We believe that the zonal electric field of intensity around 0.5 to
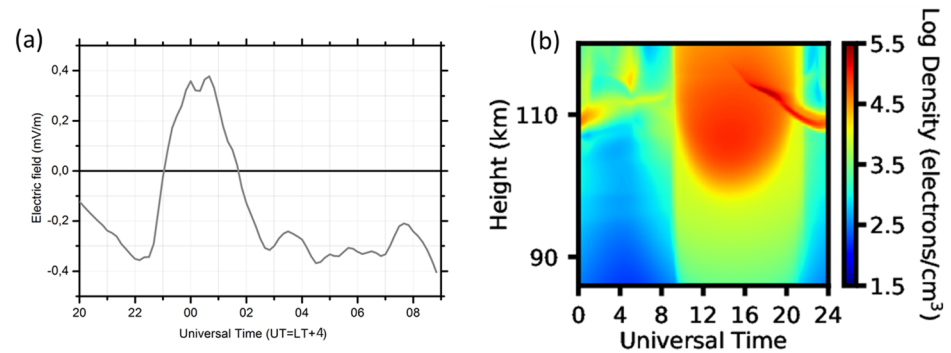
Figure 10. (a) Zonal electric profile between 2000 UT and 0900 UT on 21–22 January 2016 and (b) the electron density as a function of Universal Time (UT) versus height (km) simulated by MIRE considering the winds and the zonal electric field in (a) on BV.

1 mV/m may have driven plasma densification, as proposed by Dagar et al. (1977). In their analysis, zonal electric fields smaller than 2 mV/m, even with the influence of the winds, could form Es layers.

We analyzed the electric field evolution obtained by the vertical drift depicted in Figure 6. For each value between 2000 UT and 0000 UT, and from 0000 UT to 0600 UT, the electric field using the relationship provided by Fejer and Scherliess (1995) was computed, leading to the result presented in Figure 10a. Notice that the negative and positive values indicate, respectively, the westward and eastward polarity. Figure 10b shows the simulation results obtained from MIRE with the aforementioned electric field. It is possible to verify that the Es layer was strong during almost the entire day when compared to the reference scenario in Figure 9a. In some hours during the daytime, the Es layer disappeared, but our focus is around the night-time. The Es layer seems to be weakened around 0400 UT to 0600 UT, but right after it became strong again. This result shows that the PRE inhibition due to the DDEF can enhance the Es layer density in our simulations. We believe that this behavior did not occur in CG because the vertical drift was smaller than that of BV, and the electric field was not enough to strengthen the Es layers. Furthermore, the tidal wind configuration in CG is entirely different concerning BV, which may also have influenced the absence of the Es layers. Notice that we have not carried out a more in-depth analysis for CG because the GSWM-00 is not efficient in forming Es layers far away from the geographical equator (Resende et al., 2017a).

Finally, although there is convincing evidence that the direct DDEF might be influencing the Es layer intensification in BV during this event, the proposal of Abdu et al. (2014) cannot be discarded. The vertical electric fields mapped from the equatorial *F* region to low latitudes can have some influence on the Es layer formation in BV. However, in our study, the Es layers appear to be stronger than those observed in Abdu et al. (2014), even though BV is outside the SAMA region. Besides that, the zonal electric field values used in the previous analysis (Dagar et al., 1977) are similar to those of our study, corroborating that the intensifications observed might be associated with DDEF. Furthermore, using simulations for the first time, it was possible to verify that these strong layers in BV on 21–22 January 2016 are a consequence of the combined effect of these electric fields with the winds. Therefore, there is a considerable indication that the anomalous Es layers that occurred in BV during the recovery phase of the other six magnetic storms could also be caused by the DDEF action. Lastly, it is noteworthy that the electric field influence in the Es layers is a particularity of regions such as Brazil, which has the magnetic equator crossing the country from west to east.

4. Conclusions

Strong Es layers were observed in the ionograms obtained in BV, a low-latitude region of Brazil, during the recovery phases of magnetic storms that occurred in 2016 and 2017. A broad literature review was conducted, and it turns out that the existing works do not provide an acceptable explanation for such a strengthening. Thus, we investigated the data gathered from BV station during the days around the magnetic storm that occurred on 20 January 2016, scrutinizing the possible effects that can account for that behavior. An analysis of the ionospheric data was conducted, and the results were compared with simulations obtained from MIRE model, leading to the following main conclusions:

1. Atypical Es layers were observed on 21–22 January 2016, a period that encompasses the recovery phase of a magnetic storm. In these days, the digisonde data show the inhibition of the vertical drift *F* region PRE, giving strong evidence that the effect of the disturbed dynamo was present. The weakening of the EIA crest near sunset time seen in TEC maps over South America confirmed this assumption. The disturbance dynamo, in turn, created a zonal westward electric field in the ionosphere.

2. To further support the claim that the DDEF is the most probable cause of the atypical Es layer, two other events were analyzed using TEC maps. In both cases, it was observed weakening of the EIA after sunset, which provided evidence that the zonal westward electric field caused by a DDEF was present during the occurrence of the strong Es layers.

3. Abdu et al. (2014) affirm that the regions near of SAMA center shows the most intensified Es layer since the energetic particle precipitation process is effective. However, the Es layers observed in this study are stronger than those observed in Abdu et al. (2014), even though BV is outside of SAMA influence. This fact corroborates with our hypothesis that the DDEF was the principal agent responsible for the formation of the strong Es layer observed in BV during the studied magnetic storms.

4. In an attempt to confirm the DDEF effect in the Es layers, simulations using MIRE were performed. We included in this model the disturbed electric field, computed using the vertical drift, and the GSWM-00 model, which provides the wind components. The results showed that a constant westward electric field equal to 0.5 mV/m or an evolution of the electric fields along the day caused a significant Es layer density enhancement in the simulations as compared to the reference scenario with only the winds. This behavior supports our assumption that the DDEF leads the observed Es layer strengthening.

5. Using simulations for the first time, it was possible to verify that these strong layers in BV during the magnetic storm that occurred on 20 January 2016 are a consequence of the combined effect of the electric fields and winds. The results from the model and observations seem to contribute significantly to advance our understanding of the role of the electric fields in the Es layer formation at low latitudes. Thus, it is noteworthy that the influence of the electric fields in the Es layers is a particularity of regions such as Brazil, which has the magnetic equator crossing the country from west to east.

6. Finally, there is an indication that the DDEF action could also cause the anomalous Es layers that occurred in BV during the recovery phase of all analyzed magnetic storms. However, further study is required to compute the statistical behavior of such occurrences, which will be performed when the data are available.

Data Availability Statement

The Digisonde data from Boa Vista and TEC data can be downloaded upon registration at the Embrace webpage from INPE Space Weather Program in the following link: http://www2.inpe.br/climaespacial/portal/en/.

References

Abdu, M. A. (1997). Major phenomena of the equatorial ionosphere-thermosphere system under disturbed conditions. *Journal of Atmospheric and Terrestrial Physics*, *59*(13), 1505–1519. https://doi.org/10.1016/S1364-6826(96)00152-6

Abdu, M. A., Batista, I. S., Brum, G. M., MacDougall, J. W., Santos, A. M., de Souza, J. R., & Sobral, J. H. A. (2010). Solar flux effects on the equatorial evening vertical drift and meridional winds over Brazil: A comparison between observational data and the IRI model and the HWM representations. *Advances in Space Research*, *46*(8), 1078–1085. https://doi.org/10.1016/j.asr.2010.06.009

Abdu, M. A., Batista, I. S., Muralikrishna, P., & Sobral, J. H. A. (1996). Long term trends in sporadic *E* layers and electric fields over Fortaleza, Brazil. *Geophysical Research Letters*, *23*(7), 757–760. https://doi.org/10.1029/96GL00589

Abdu, M. A., Batista, I. S., Reinisch, B. W., de Souza, J. R., Sobral, J. H. A., Pedersen, T. R., & Groves, K. M. (2009). Conjugate Point Equatorial Experiment (COPEX) campaign in Brazil: Electrodynamics highlights on spread development conditions and day-to-day variability. *Journal of Geophysical Research: Space Physics*, *114*, A04308. https://doi.org/10.1029/2008ja013749

Abdu, M. A., & Brum, G. M. (2009). Electrodynamics of the vertical coupling processes in the atmosphere-ionosphere system of the low latitude region. *Earth, Planets and Space*, *61*(4), 385–395. https://doi.org/10.1186/BF03353156

Abdu, M. A., de Souza, J. R., Batista, I. S., Santos, M. A., Sobral, J. H. A., Rastogi, R. G., & Chandra, H. (2014). The role of electric fields in sporadic *E* layer formation over low latitudes under quiet and magnetic storm conditions. *Journal of Atmospheric and Terrestrial Physics*, *115-116*, 95–105. https://doi.org/10.1016/j.jastp.2013.12.003

Abdu, M. A., de Souza, J. R., Sobral, J. H. A., & Batista, I. S. (2006). Magnetic storm associated disturbance dynamo effects in the low and equatorial latitude ionosphere, in recurrent magnetic storms: Corotating solar wind streams. *Geophysical Monograph Series*, *167*, 283–304. https://doi.org/10.1029/167GM22

Abdu, M. A., MacDougall, J. W., Batista, I. S., Sobral, J. H. A., & Jayachandran, P. T. (2003). Equatorial evening prereversal electric field enhancement and sporadic *E* layer disruption: A manifestation of *E* and *F* region coupling. *Journal of Geophysical Research: Space Physics*, *108*(A6), 1254. https://doi.org/10.1029/2002JA009285

Arras, C., Wickert, J., Beyerle, G., Heise, S., Schmidt, T., & Jacobi, C. (2008). A global climatology of ionospheric irregularities derived from GPS radio occultation. *Geophysical Research Letters*, *35*(14), L14809. https://doi.org/10.1029/2008GL034158

Balan, N., Alleyne, H., Walker, S., Reme, H., McCrea, I., & Aylward, A. (2008). Magnetosphere-ionosphere coupling during the CME events of 07–12 November 2004. *Journal of Atmospheric and Terrestrial Physics*, *70*(17), 2101–2111. https://doi.org/10.1016/j.jastp.2008.03.015

Batista, I. S., Abdu, M. A., Carrasco, A. J., Reinisch, B. W., de Paula, E. R., Schuch, N. J., & Bertoni, F. (2008). Equatorial spread *F* and sporadic *E*-layer connections during the Brazilian Conjugate Point Equatorial Experiment (COPEX). *Journal of Atmospheric and Solar-Terrestrial Physics*, *70*(8–9), 1133–1143. https://doi.org/10.1016/j.jastp.2008.01.007

Batista, I. S., Candido, C. M. N., Souza, J. R., Abdu, M. A., de Araujo, R. C., Resende, L. C. A., & Santos, A. M. (2017). *F3* layer development during quiet and disturbed periods as observed at conjugate locations in Brazil: The role of the meridional wind. *Journal of Geophysical Research: Space Physics*, *122*(2), 2361–2373. https://doi.org/10.1002/2016JA023724

Bishop, R. L., & Earcle, G. D. (2003). Metallic ion transport associated with midlatitude intermediate layer development. *Journal of Geophysical Research: Space Physics*, *108*(A1), 1019. https://doi.org/10.1029/2002JA009411

Bittencourt, J. A., & Abdu, M. A. (1981). A theoretical comparison between apparent and real vertical ionization drift velocities in the equatorial *F* region. *Journal of Geophysical Research: Space Physics*, *86*(A4), 2451–2454. https://doi.org/10.1029/JA086iA04p02451

Blanc, M., & Richmond, A. D. (1980). The ionospheric disturbance dynamo. *Journal of Geophysical Research: Space Physics*, *85*(A4), 1669–1686. https://doi.org/10.1029/JA085iA04p01669

Buriti, R. A., Hocking, W. K., Batista, P. P., & Medeiros, A. F. (2008). Observations of equatorial mesospheric winds over Cariri (7.4°S) by a meteor radar and comparison with existing models. *Annales Geophysicae*, *26*(3), 485–497. https://doi.org/10.5194/angeo-26-485-2008

Carrasco, A. J., Batista, I. S., & Abdu, M. A. (2007). Simulation of the sporadic *E* layer response to pre-reversal associated evening vertical electric field enhancement near dip equator. *Journal of Geophysical Research: Space Physics*, A06324. https://doi.org/10.1029/2006JA012143

Da Silva, L. A., Satyamurty, P., Alves, L. R., Souza, V. M., Jauer, P. R., Silveira, M. V. D., & Vieira, L. E. A. (2016). Comparison of geophysical patterns in the southern hemisphere mid-latitude region. *Advances in Space Research*, *58*(10), 2090–2103. https://doi.org/10.1016/j.asr.2016.04.003

Dagar, R., Verma, P., Napgal, O., & Setty, C. S. G. K. (1977). The relative effects of electric fields and neutral winds on the formation of the equatorial sporadic layers. *Annales Geophysicae*, *33*(3), 333–340.

Denardini, C. M., Dasso, S., & Gonzalez-Esparza, J. A. (2016). Review on space weather in Latin America. 2. The research networks ready for space weather. *Advances in Space Research*, *58*(10), 1940–1959. https://doi.org/10.1016/j.asr.2016.03.013

Fejer, B. G., Jensen, J. W., & Su, S. Y. (2008). Seasonal and longitudinal dependence of equatorial disturbance vertical plasma drifts. *Geophysical Research Letters*, *35*, L20106. https://doi.org/10.1029/L035584

Fejer, B. G., & Scherliess, L. (1995). Time dependent response of equatorial ionospheric electric fields to magnetospheric disturbances. *Geophysical Research Letters*, *22*(7), 851–854. https://doi.org/10.1029/95gl00390

Fürst, F., Wilms, J., Rothschild, R. E., Pottschmidt, K., Smith, D. M., & Lingenfelter, R. (2009). Temporal variations of strength and location of the South Atlantic anomaly as measured by RXTE. *Earth and Planetary Science Letters*, *281*(3-4), 125–133. https://doi.org/10.1016/j.epsl.2009.02.004

Ginet, G. P., Madden, D., Dichter, B. K., and Brautigam, G. D. H. (2007). Energetic proton maps for the South Atlantic anomaly. *IEEE Radiation Effects Data Workshop*, Honolulu, HI, USA, 23–27 July 2007.

Gonzalez, W. D., Joselyn, J. A., Kamide, Y., Kroehl, H. W., Rostoker, G., Tsurutani, B. T., & Vasyliunas, V. M. (1994). What is a magnetic storm? *Journal of Geophysical Research: Space Physics*, *99*(A4), 5771–5792. https://doi.org/10.1029/93JA02867

Hagan, M. E., & Forbes, J. M. (2002). Migrating and nonmigrating diurnal tides in the middle and upper atmosphere excited by tropospheric latent heat release. *Journal of Geophysical Research: Space Physics*, *107*(D24), 4754. https://doi.org/10.1029/2001JD001236

Hagan, M. E., & Forbes, J. M. (2003). Migrating and nonmigrating semidiurnal tides in the upper atmosphere excited by tropospheric latent heat release. *Journal of Geophysical Research: Space Physics*, *108*(A2), 1062. https://doi.org/10.1029/2002JA009466

Haldoupis, C. (2011). A tutorial review on sporadic *E* layers, Aeronomy of the Earth's atmosphere-ionosphere. *IAGA Book Series*, *29*(2), 381–394. https://doi.org/10.1007/978-94-007-0326-1_29

Haldoupis, C., Meek, C., Christakis, N., Pancheva, D., & Bourdillon, A. (2006). Ionogram height-time intensity observations of descending sporadic *E* layers at mid-latitude. *Journal of Atmospheric and Terrestrial Physics*, *68*(3-5), 539–557. https://doi.org/10.1016/j.jastp.2005.03.020

Hedin, A. E., Biondi, M. A., Burnside, R. G., Hernadez, G., Johson, R. M., Killen, T. L., et al. (1991). Revised global model of thermosphere winds using a satellite and ground-based observations. *Journal of Geophysical Research*, *96*(A5), 7657–7688. https://doi.org/10.1029/91JA00251

Kennel, C. F., & Petschek, H. E. (1966). Limit on stably trapped particle fluxes. *Journal of Geophysical Research*, *71*(1), 1–28. https://doi.org/10.1029/JZ071i001p00001

Kopp, E. (1997). On the abundance of metal ions in the lower ionosphere. *Journal of Geophysical Research*, *102*, 9667–9674. https://doi.org/10.1029/97ja00384

Mathews, J. D. (1998). Sporadic *E*: Current views and recent progress. *Journal of Atmospheric and Terrestrial Physics*, *60*(4), 413–435. https://doi.org/10.1016/S1364-6826(97)00043-6

Mauk, B. H., Fox, N. J., Kanekal, S. G., Kessel, R. L., Sibeck, D. G., & Ukhorskiy, A. (2012). Science objectives and rationale for the radiation belt storm probes mission. *Space Science Reviews*, *179*(1-4), 3–27. https://doi.org/10.1007/s11214-012-9908-y

Moro, J., Resende, L. C. A., Denardini, C. M., Xu, J., Batista, I. S., Andrioli, V. F., & Schuch, N. J. (2017). Equatorial *E* region electric fields and sporadic *E* layer responses to the recovery phase of the November 2004 geomagnetic storm. *Journal of Geophysical Research: Space Physics*, *122*(12), 12,517–12,533. https://doi.org/10.1002/2017JA024734

Nogueira, P. A. B., Abdu, M. A., Batista, I. S., & Siqueira, P. M. (2011). Equatorial ionization anomaly and thermospheric meridional winds during two major storms over Brazilian low latitudes. *Journal of Atmospheric and Solar-Terrestrial Physics*, *73*(11-12), 1535–1543. https://doi.org/10.1016/j.jastp.2011.02.008

Otsuka, Y., Ogawa, T., Saito, A., Tsugawa, T., Fukao, S., & Miyazaki, S. (2002). A new technique for mapping of total electron content using GPS network in Japan. *Earth, Planets and Space*, *54*(1), 63–70. https://doi.org/10.1186/BF03352422

Pignalberi, A., Pezzopane, M., & Zuccheretti, E. (2014). Sporadic *E* layer at mid-latitudes: average properties and influence of atmospheric tides. *Annales Geophysicae*, *32*, 1427–1440. https://doi.org/10.5194/angeo-32-1427-2014

Prasad, S. N. V. S., Prasad, D. S. V. V. D., Venkatesh, K. K., Niranjan, K., & Rama Rao, P. V. S. (2012). Diurnal and seasonal variations in sporadic *E*-layer (Es layer) occurrences over equatorial, low and mid latitude stations—A comparative study. *Indian Journal of Radio & Space Physics*, *41*, 26–35.

Rastogi, R. G., Chandra, H., Condori, L., Abdu, M. A., Reinisch, B., Tsunoda, R. T., et al. (2012). Abnormally large magnetospheric electric field on 9 November 2004 and its effect on equatorial ionosphere around the world. *Journal of Earth System Science*, *121*(5), 1145–1161. https://doi.org/10.1007/s12040-012-0231-5

Reinisch, B. W., Galkin, I. A., & Khmyrov, G. M. (2009). The new Digisonde for research and monitoring applications. *Radio Science*, *44*, RS0A24. https://doi.org/10.1029/2008RS004115

Reinisch, B. W., Galkin, I. A., Khmyrov, G. M., Kozlov, A., & Kitrosser, D. (2004). Automated collection and dissemination of ionospheric data from the Digisonde network. *Advances in Radio Science*, *2*, 241–247. https://doi.org/10.5194/ars-2-241-2004

Resende, L. C. A., Batista, I. S., Denardini, C. M., Batista, P. P., Carrasco, A. J., Andrioli, V. F., & Moro, J. (2017a). Simulations of blanketing sporadic *E*-layer over the Brazilian sector driven by tidal winds. *Journal of Atmospheric and Solar-Terrestrial Physics*, *154*, 104–114. https://doi.org/10.1016/j.jastp.2016.12.012

Resende, L. C. A., Batista, I. S., Denardini, C. M., Batista, P. P., Carrasco, A. J., Andrioli, V. F., & Moro, J. (2017b). The influence of tidal winds in the formation of blanketing sporadic *E*-layer over equatorial Brazilian region. *Journal of Atmospheric and Solar-Terrestrial Physics*, *171*, 64–71. https://doi.org/10.1016/j.jastp.2017.06.009

Resende, L. C. A., Batista, I. S., Denardini, C. M., Carrasco, A. J., Andrioli, V. F., Moro, J., et al. (2016). Competition between winds and electric fields in the formation of blanketing sporadic *E* layers at equatorial regions. *Earth, Planets and Space*, *68*(1), 201. https://doi.org/10.1186/s40623-016-0577-z

Resende, L. C. A., Denardini, C. M., & Batista, I. S. (2013). Abnormal fbEs enhancements in equatorial Es layers during magnetic storms of solar cycle 23. *Journal of Atmospheric and Solar-Terrestrial Physics*, *102*, 228–234. https://doi.org/10.1016/j.jastp.2013.05.020

Rishbeth, H., Ganguly, S., & Walker, J. C. G. (1978). Field-aligned and field-perpendicular velocities in ionospheric *F*2-layer. *Journal of Atmospheric and Solar-Terrestrial Physics*, *40*(7), 767–784. https://doi.org/10.1016/0021-9169(78)90028-4

Santos, A. M., Abdu, M. A., Sobral, J. H., Koga, D., Nogueira, P. A. B., & Candido, C. M. N. (2012). Strong longitudinal difference in ionospheric responsesover Fortaleza (Brazil) and Jicamarca (Peru) during the January 2005 magnetic storm, dominated by northward IMF. *Journal of Geophysical Research: Space Physics*, *117*, A08333. https://doi.org/10.1029/2012JA017604

Santos, A. M., Abdu, M. A., Souza, J. R., Sobral, J. H., Batista, I. S., & Denardini, C. M. (2016). Stormtime equatorial plasma bubble zonal drift reversal due to disturbance hall electric field over the Brazilian region: Disturbed zonal plasma drift. *Journal of Geophysical Research: Space Physics*, *121*(6), 5594–5612. https://doi.org/10.1002/2015JA022179

Sastri, J. H. (1988). Equatorial electric fields of ionospheric disturbance dynamo origin. *Annales Geophysicae*, *6*, 635–642.

Singh, R., & Sripathi, S. (2020). A statistical study on the local time dependence of equatorial spread *F* (ESF) irregularities and their relation to low-latitude Es layers under geomagnetic storms. *Journal of Geophysical Research: Space Physics*, *125*. https://doi.org/10.1029/2019JA027212

Takahashi, H., Wrasse, C. M., Denardini, C. M., Pádua, M. B., de Paula, E. R., Costa, S. M. A., et al. (2016). Ionospheric TEC weather map over South America. *Space Weather*, *14*(11), 937–949. https://doi.org/10.1002/2016SW001474

Thorne, R. M. (2010). Radiation belt dynamics: The importance of wave-particle interactions. *Geophysical Research Letters*, *37*(22), L22107. https://doi.org/10.1029/2010GL044990

Whitehead, J. (1961). The formation of the sporadic-*E* in the temperate zones. *Journal of Atmospheric and Terrestrial Physics*, *20*(1), 49–58. https://doi.org/10.1016/0021-9169(61)90097-6